Optics Communications 522 (2022) 128695

Contents lists available at ScienceDirect

Optics Communications

journal homepage: www.elsevier.com/locate/optcom

Group delay and spectral phase retrieval of light pulses by spectral intensity measurements

C. Cuadrado-Laborde [b,*], J.L. Cruz [a], A. Díez [a], M.V. Andrés [a]

[a] Departamento de Física Aplicada, ICMUV, Universidad de Valencia, Dr. Moliner 50, Burjassot E-46100, Spain
[b] Instituto de Física Rosario (CONICET-UNR), Blvr. 27 de Febrero 210bis, S2000EZP, Rosario, Argentina

ARTICLE INFO

Keywords:
Phase-recovery
Fiber optics
Fiber lasers
Fourier transform
Photonics signal processing

ABSTRACT

We discuss a method to determine both the group delay and the phase of a given pulse in the Fourier optics domain. The proposal is based on the measurement of two intensity spectra, before and after a known quadratic phase modulation. A simple analytical equation is then used to determine the group delay in one step. If necessary, the spectral phase can be determined by simple spectral integration of the determined group delay. The proposal is supported by various numerical results and an experimental measurement to prove the concept.

1. Introduction

The electric field of an optical pulse can be described in the time domain or in the frequency domain. In the frequency domain, it may be of interest to know not only the intensity spectrum, but also the spectral phase, which contains additional and complementary information. In the Fourier representation of signals, the spectral magnitude and the spectral phase play different roles and in some situations many of the important features of a signal are preserved even if only the spectral phase is retained [1–3]. This was illustrated by the following numerical experiment: two different images were Fourier transformed. The phases of their Fourier transforms were swapped and then they were inverse Fourier transformed. Surprisingly, the images obtained were associated with the swapped phases and not with the correct magnitudes. This simple numerical example shows that the spectral phase contains a considerable amount of information. Moreover, under various conditions, such as when a signal is of finite duration, the phase information alone is sufficient to reconstruct a signal to within a scale factor [4].

However, in a typical optical spectrum analyzer, only the intensity spectrum is measured, and the spectral phase information is completely lost. On the contrary, the spectral phase or its first-order derivative, the group delay, can be obtained by more sophisticated methods such as frequency-resolved optical gating (FROG) [5] or spectral phase interferometry for direct reconstruction of the electric-field (SPIDER) [6]. Although their efficiency is beyond question, both methods are best suited for short or ultrashort light pulses above a certain power threshold. Later, it was proposed TADPOLE (Temporal Analysis, by Dispersing a Pair Of Light *E*-fields) for characterizing weak ultrashort laser pulses [7], but still relying in a well-characterized and more energetic reference pulse by using a combination of FROG and spectral interferometry. Finally, we should mention here also the dispersion scan technique (*d-scan*) which also relies in a nonlinear effect, the second harmonic generation [8].

The task of recovering a signal from its phaseless Fourier transform amplitude is called Fourier phase recovery and appears in many different branches of science [9]. In a few words, it could be expressed as follows: although there is a clear Fourier transform relation between the complex signal in the time and spectral domains, no such relation seems to exist for the intensities [10]. It is concluded that one cannot expect to uniquely determine the phase in any domain from the signal modulus in that domain. Various solutions have therefore been proposed. One particularly successful solution is the Gerchberg–Saxton algorithm (GSA) [11]. The GSA is an iterative algorithm for determining the phase of a complex-valued signal from the intensity waveforms in the time and Fourier domains. The algorithm starts by proposing a random phase and repeatedly goes back and forth between the two domains through the Fourier/anti-Fourier transforms, keeping the phases and replacing the calculated amplitudes with the measured ones to obtain the final phases in both domains. This iterative process is of course time consuming and its results are also sensitive in some cases to finding an educated guess for the initial phase.

In Ref. [12], we proposed a simple and fast procedure to obtain the temporal phase profile of any light pulse by recovering the instantaneous frequency. The proposal required only the measurement of the temporal intensity waveforms before and after a given propagation length with known group velocity dispersion. This proposal was used, for example, in the first experimental measurement of the instantaneous frequency profile of a dissipative resonant light pulse (DSR) [13]. Our work could be considered as the temporal counterpart of the earlier

* Corresponding author at: Instituto de Física Rosario (CONICET-UNR), Blvr. 27 de Febrero 210bis, S2000EZP, Rosario, Argentina.
E-mail address: cuadradolaborde@ifir-conicet.gov.ar (C. Cuadrado-Laborde).

https://doi.org/10.1016/j.optcom.2022.128695
Received 11 January 2022; Received in revised form 14 June 2022; Accepted 27 June 2022
Available online 30 June 2022

work by Dorrer and Kang [14]. In that work, the authors derived an expression relating the group delay to two intensity spectra, before and after a known time squared phase modulation, from a small shear along the frequency axis in the Wigner–Ville distribution [15,16]. However, although the power of the Wigner–Ville distribution function is beyond question, it is no less true that not all researchers working in this area are sufficiently familiar with this formalism. In this article we present a novel derivation of the group delay measurement method, first proposed in Ref. [14]. Our derivation is relatively simple and requires only modest handling of some fundamental properties of the Fourier transform. Moreover, our experimental setup is specifically designed for passively modelocked lasers, while in Ref. [14] it was specifically designed for actively modelocked lasers, where a clock signal is readily available.

In what follows, we provide a theoretical analysis of the problem (Section 2). In Section 3, we test this proposal numerically under several scenarios, including: the interrogation of the spectral phase profile of a linearly chirped Gaussian pulse with and without noise, the influence of the quadratic phase modulation factor, and the success of phase interrogation for nonlinear chirps. In Section 4, we discuss the results of a proof-of-concept experiment to recover the group delay of a transform-limited soliton after a certain dispersive propagation. Finally, in Section 5 we summarize the main conclusions of this work.

2. Theory

Suppose a given light pulse, which in the time domain can be expressed as a one-dimensional complex signal $f(t) = |f(t)| \exp[j\varphi(t)]$; while in the spectral domain it can be expressed via the Fourier transform ($\mathfrak{F}$) as $F(\omega) = |F(\omega)| \exp[j\Phi(\omega)]$, where ω is the baseband angular frequency. In the Fourier domain, we can define the group delay as the spectral derivative of the phase $d\Phi(\omega)/d\omega = \Phi'(\omega)$, which can be written in terms of the signal itself as follows:

$$\Phi'(\omega) = \mathrm{Im}\frac{\mathrm{d}\ln F(\omega)}{\mathrm{d}\omega} = \mathrm{Im}\frac{F'(\omega)}{F(\omega)} = \frac{j}{2}\left[\frac{F'^{*}(\omega)}{F^{*}(\omega)} - \frac{F'(\omega)}{F(\omega)}\right] \tag{1}$$

where from now on the prime above a function indicates a spectral derivative, while the asterisk denotes the complex conjugation. Thus we obtain the following relation:

$$\Phi'(\omega)\,|F(\omega)|^2 = \frac{j}{2}\left[F'^{*}(\omega)\,F(\omega) - F^{*}(\omega)\,F'(\omega)\right]. \tag{2}$$

Let us now turn to a quadratic phase modulation, currently known as the time lens $l(t)$ [17,18], which can be expressed in the time and frequency domains as follows:

$$l(t) = \exp\left(\frac{j}{2}\phi_{20}t^2\right) \xrightarrow{\mathfrak{F}} L(\omega) \propto \exp\left(-\frac{j}{2}\frac{\omega^2}{\phi_{20}}\right), \tag{3}$$

where ϕ_{20} is the quadratic phase modulation factor in rad × Hz^2. Therefore, a given signal $f(t)$ after a quadratic phase modulation can be expressed in the time domain as follows:

$$f_{\phi_{20}}(t) = f(t)\exp\left(\frac{j}{2}\phi_{20}t^2\right), \tag{4}$$

where $f_{\phi_{20}}(t)$ is the quadratic phase modulated signal. In the spectral domain, Eq. (4) can be expressed as a convolution as follows:

$$F_{\phi_{20}}(\omega) = \int_{-\infty}^{\infty}\mathrm{d}\varpi\,F(\varpi)\exp\left[-\frac{j}{2}\frac{(\omega-\varpi)^2}{\phi_{20}}\right]. \tag{5}$$

Using Eq. (5) and after some algebraic manipulations, we can show the following relation, which we will find very useful immediately following:

$$\frac{\partial F_{\phi_{20}}(\omega)}{\partial\phi_{20}} \cong -\frac{j}{2}\frac{\mathrm{d}^2F_{\phi_{20}}(\omega)}{\mathrm{d}\omega^2}. \tag{6}$$

Now, if you calculate the derivative of the quadratic modulus of the quadratic phase-modulated spectrum respect to ϕ_{20}:

$$\frac{\partial\left|F_{\phi_{20}}(\omega)\right|^2}{\partial\phi_{20}} = \frac{\partial\left[F^{*}_{\phi_{20}}(\omega)\,F_{\phi_{20}}(\omega)\right]}{\partial\phi_{20}} = \frac{\partial F^{*}_{\phi_{20}}(\omega)}{\partial\phi_{20}}F_{\phi_{20}}(\omega) + F^{*}_{\phi_{20}}(\omega)\frac{\partial F_{\phi_{20}}(\omega)}{\partial\phi_{20}}, \tag{7}$$

and substituting Eq. (6) in (7), this leads to:

$$\frac{\partial\left|F_{\phi_{20}}(\omega)\right|^2}{\partial\phi_{20}} = \frac{j}{2}\left[F_{\phi_{20}}(\omega)F''^{*}_{\phi_{20}}(\omega) - F^{*}_{\phi_{20}}(\omega)F''_{\phi_{20}}(\omega)\right], \tag{8}$$

which can be easily converted to:

$$\frac{\partial\left|F_{\phi_{20}}(\omega)\right|^2}{\partial\phi_{20}} = \frac{j}{2}\frac{\mathrm{d}}{\mathrm{d}\omega}\left[F_{\phi_{20}}(\omega)F'^{*}_{\phi_{20}}(\omega) - F^{*}_{\phi_{20}}(\omega)F'_{\phi_{20}}(\omega)\right] \tag{9}$$

Although the expressions between the square brackets in Eqs. (2) and (9) are different a priori, they can be made equal if $\phi_{20}\to 0$. Since in that case, the action of the time lens is null, see Eq. (3), therefore $F_{\phi_{20}}(\omega)\big|_{\phi_{20}\to 0} = F(\omega)$, $F'^{*}_{\phi_{20}}(\omega)\big|_{\phi_{20}\to 0} = F'^{*}(\omega)$, $F^{*}_{\phi_{20}}(\omega)\big|_{\phi_{20}\to 0} = F^{*}(\omega)$, and $F'_{\phi_{20}}(\omega)\big|_{\phi_{20}\to 0} = F'(\omega)$. Therefore:

$$F'^{*}(\omega)\,F(\omega) - F^{*}(\omega)\,F'(\omega) = \left[F_{\phi_{20}}(\omega)F'^{*}_{\phi_{20}}(\omega) - F^{*}_{\phi_{20}}(\omega)F'_{\phi_{20}}(\omega)\right]\Big|_{\phi_{20}\to 0}. \tag{10}$$

Thus, by combining Eqs. (2) and (9) and considering Eq. (10), we obtain:

$$\frac{\mathrm{d}\left[\Phi'(\omega)\,|F(\omega)|^2\right]}{\mathrm{d}\omega} = \frac{\partial\left|F_{\phi_{20}}(\omega)\right|^2}{\partial\phi_{20}}\Bigg|_{\phi_{20}\to 0}. \tag{11}$$

This equation links the variations in spectral intensity due to quadratic modulation to spectral intensity and phase, and could be considered the spectral counterpart of the well-known transport-of-intensity equation. Finally, integrating over ω in Eq. (11), yields:

$$\Phi'(\omega)\,|F(\omega)|^2 = \int_{-\infty}^{\omega}\frac{\partial\left|F_{\phi_{20}}(\varpi)\right|^2}{\partial\phi_{20}}\Bigg|_{\phi_{20}\to 0}d\varpi, \tag{12}$$

which can be easily transformed into:

$$\Phi'(\omega) = \frac{1}{|F(\omega)|^2}\int_{-\infty}^{\infty}\frac{\partial\left|F_{\phi_{20}}(\varpi)\right|^2}{\partial\phi_{20}}\Bigg|_{\phi_{20}\to 0}H(\omega-\varpi)\,d\varpi, \tag{13}$$

where $H(.)$ is the Heaviside step function. Eq. (13) is the main result of this work, and states that the group delay of the signal can be obtained by convolving the derivative of the spectral signal intensity by the quadratic phase modulation factor ϕ_{20} with the Heaviside step function. Eq. (13) is essentially the same as the equation first derived by Dorrer and Kang, see Eq. (5) in Ref. [14], although in this case was obtained by a simpler route. Moreover, this equation can be viewed as the spectral version of the general formulation first derived by Bastiaans and Wolf for unitary canonical transformations [19]. Finally, the phase in the spectral domain can be obtained by simply integrating the angular frequency; i.e.:

$$\Phi(\omega) = \int_{-\infty}^{\omega}\Phi'(\varpi)\,d\varpi \tag{14}$$

Regarding the derivation of the quadratic phase-modulated intensity spectrum, see Eq. (13), we propose the following approximation:

$$\frac{\partial\left|F_{\phi_{20}}(\omega)\right|^2}{\partial\phi_{20}}\Bigg|_{\phi_{20}\to 0} \approx \frac{\left|F_{\phi_{20}}(\omega)\right|^2 - |F(\omega)|^2}{\phi_{20}}\Bigg|_{\phi_{20}\to 0}, \tag{15}$$

i.e., we replace the computation of the derivative by a finite difference. Of course, the approximation given by Eq. (15) improves when the phase modulation factor ϕ_{20} approaches zero. Experimentally, however, we have to find a compromise between using a low ϕ_{20} value on the one hand and a good signal to noise ratio in the signal difference on the other hand, see Eq. (15). For a detailed discussion on the use of phase modulators as time lenses with practical implications, see the Refs. [20,21]. Finally, we emphasize the ability of this technique to characterize low power signals, due to the high sensitivity and dynamic range of standard optical spectrum analyzers required to measure both signal spectra in Eq. (15) (typically above −75 dBm).

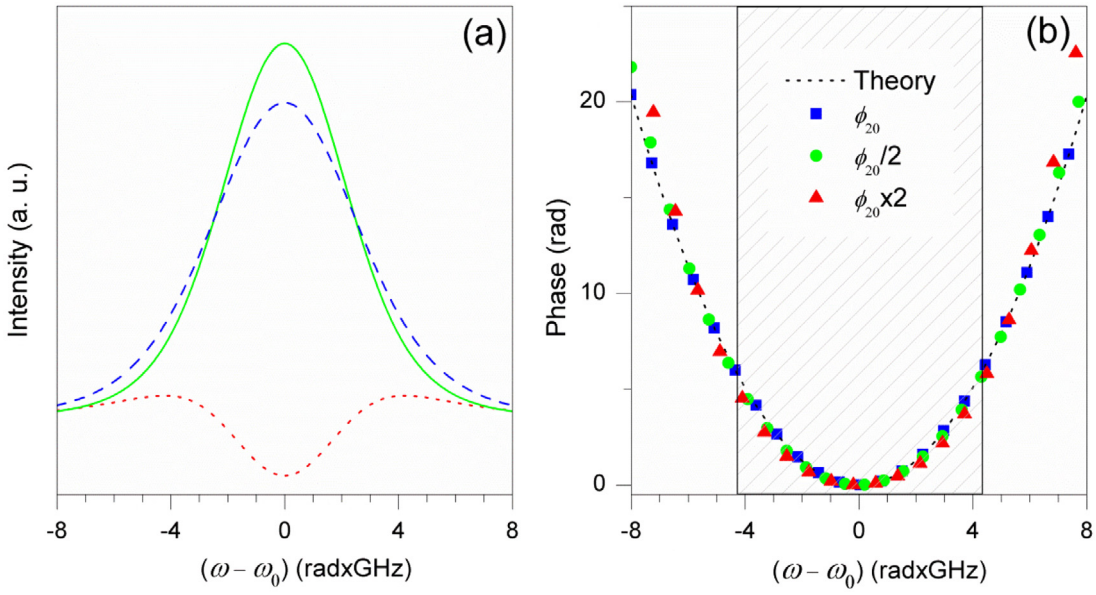

Fig. 1. (a) Intensity spectrum of the tested pulse (green solid curve), intensity spectrum of the pulse after quadratic phase modulation (blue dashed curve), and the difference between them (red dotted curve). (b) Phase retrieved with $\phi_{20} = 1.24 \times 10^{19}$ rad ×Hz^2, 2×ϕ_{20}, and 1/2×ϕ_{20}, compared to the theoretical phase; the shaded region covers 90% of the spectral tested pulse.

3. Numerical results

In this section we will focus on the aspects of the technique that were not covered in Ref. [14], in particular the recovery of non-square phase profiles and the robustness of this technique in the presence of noise. To test the performance of this proposal, we first numerically simulated the spectral phase retrieval of a linearly chirped hyperbolic secant pulse. We chose this waveform, because it occurs naturally in the context of mode-locked lasers. The optical field associated with this pulse can be expressed in the time domain as follows:

$$f(t) = \operatorname{sech}\left(\frac{t}{T_0}\right)\exp\left(-\frac{jCt^2}{2T_0^2}\right), \tag{16}$$

where T_0 is the half-width at the $1/e$ value of peak intensity, associated with T_{FWHM}, the full-width at half-maximum (FWHM), by $T_{\mathrm{FWHM}} \cong 1.763T_0$; and C is a dimensionless chirp parameter. Numerical calculations were performed in a time window of 20.47 ns with 2^{11} points equally spaced, resulting in a sampling time of 10 ps. Fig. 1(a) shows the Fourier transform in intensity, i.e. $|F(\omega)|^2$, of the pulse given by Eq. (16) with $T_{\mathrm{FWHM}} = 500$ ps and $C = 5$. This figure also shows the spectrum of the pulse after phase modulation, i.e. $\left|F_{\phi_{20}}(\omega)\right|^2$, with $\phi_{20} = 1.24 \times 10^{19}$ rad × Hz^2, and the signal difference between the two, i.e. $\left|F_{\phi_{20}}(\omega)\right|^2 - |F(\omega)|^2$, which is important for phase determination, see Eq. (15). Fig. 1(b) shows the phase recovery in the Fourier domain by using Eq. (14), with the help of Eqs. (13) and (15). For comparison purposes, the theoretically calculated phase in the spectral domain of the input light pulse is also shown, i.e. $\Phi(\omega)$. As you can see, both profiles are in complete agreement within the shaded region that encompasses 90% of the tested spectral pulse power. Finally, to show the sensitivity of this technique when the phase modulation factor is changed, we show in the same figure two other phase profiles obtained with a different phase modulation factor ϕ_{20}, i.e. double and half the value used before. As you can see, there are no significant differences between them. However, it is clear that a phase modulation factor high enough should be used to produce a signal difference above the measurement noise.

We also test the robustness of this technique by simulating additive and independent white noise before and after the quadratic phase modulation, i.e., in $|F(\omega)|^2$ and $\left|F_{\phi_{20}}(\omega)\right|^2$. In Fig. 2, we show the group delay directly recovered using Eq. (13) with the unsmoothed data for a signal-to-noise ratio (SNR) of 15 dB and 10 dB compared to the theoretical group delay [the other parameters are the same as in Fig. 1(a)]. Just as an example, we show also the signal difference at the SNR of 10 dB, see Fig. 2(b). As you can see, the group delay can be satisfactorily recovered despite the strong presence of noise. This synergistic robustness to intensity noise is related to both the inherent low-pass behavior of the integral and the replacement of the original derivative by a finite difference [see Eqs. (13) to (15)]. Of course, the spectral phase can be recovered as usual using Eq. (14). It is important to emphasize that a temporal mismatch between the pulse peak and the quadratic phase modulation in the time lens does not have a major impact [22], since it only causes a spectral shift in both the group delay and the spectral phase, which can subsequently be corrected numerically.

We conclude this section by demonstrating the applicability of this technique to a different phase profile. To this end, we simulated the recovery of the group delay of a noiseless super-Gaussian pulse defined by:

$$f(t) = \exp\left(-\frac{(1+jC)}{2}\frac{t^{2m}}{T_0^{2m}}\right), \tag{17}$$

where m is the edge sharpness parameter, C is the chirp parameter, and T_0 is related to the rise time T_r (which in turn is defined as the duration during which the intensity increases from 10% to 90%), by $T_r = T_0/m$ [23]. Fig. 3(a) shows the Fourier transform of the intensity, i.e., $|F(\omega)|^2$, of the pulse given by Eq. (17), with $T_{\mathrm{FWHM}} = 500$ ps, $C = 5$, and $m = 3$. This figure also shows the spectrum of the pulse after phase modulation, i.e. $\left|F_{\phi_{20}}(\omega)\right|^2$, with $\phi_{20} = 2.48 \times 10^{19}$ rad × Hz^2, and the signal difference between the two; i.e. $\left|F_{\phi_{20}}(\omega)\right|^2 - |F(\omega)|^2$, which is essential for phase recovery, see Eq. (15). Fig. 3(b) shows the recovered phase using Eq. (14) with the help of Eqs. (13) and (15). For comparison, the theoretically calculated phase in the spectral domain of the input light pulse is also shown; i.e. $\Phi(\omega)$. Even in this more complex case of nonlinear chirp, a reasonable degree of similarity between the two profiles is observed, especially within the shaded region that includes 80% of the tested spectral pulse power.

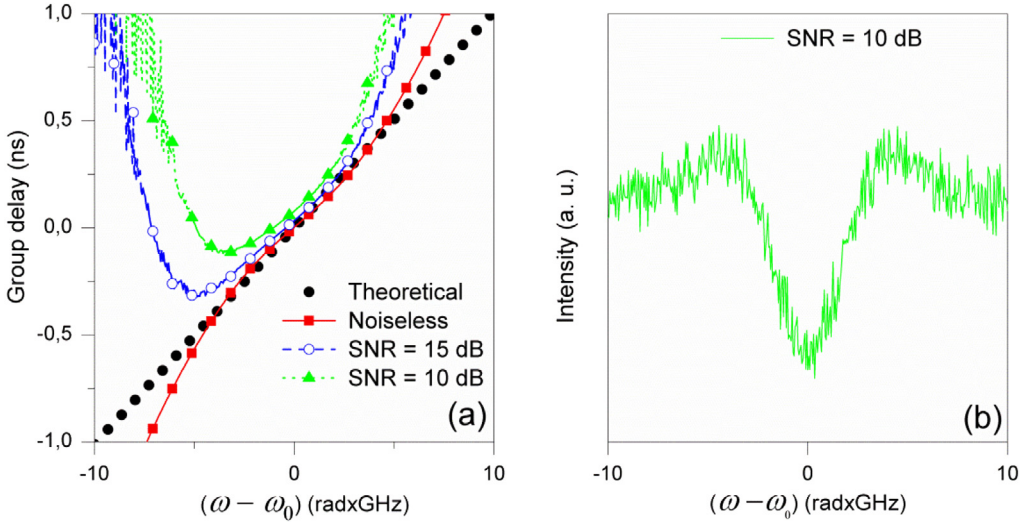

Fig. 2. (a) Recovered group delay in the presence of noise for the Gaussian chirped pulse analyzed in Fig. 1(a), when the SNR = 15 dB and 10 dB, compared with the recovered group delay without noise and the theoretical group delay. (b) Spectral signal difference used to recover the group delay, see Eq. (15), when the SNR is 10 dB.

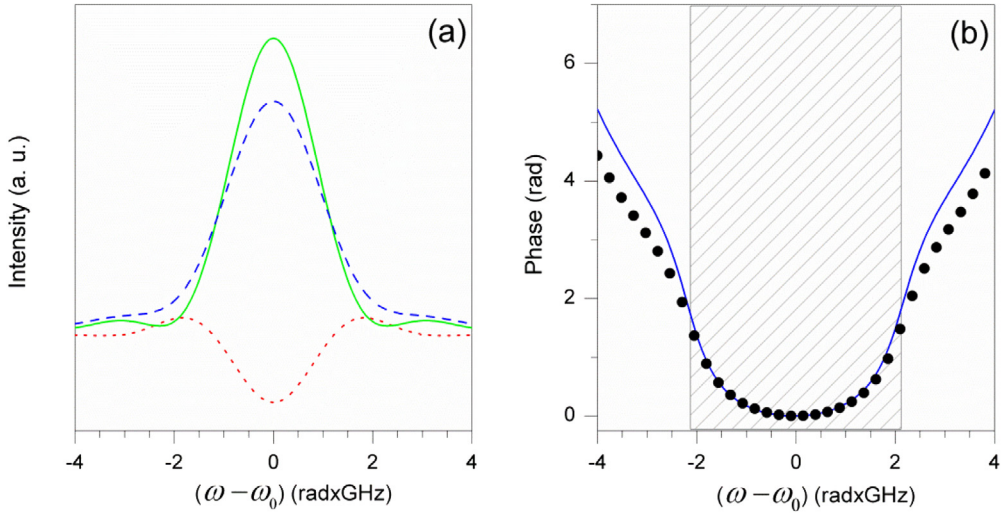

Fig. 3. (a) Intensity spectrum of the tested noiseless super-Gaussian chirped pulse (green solid curve), intensity spectrum of the pulse after quadratic phase modulation (blue dashed curve), and the difference between them (red dotted curve). (b) Spectral phase of the super-Gaussian chirped pulse compared to the theoretical phase (blue solid curve and solid scatter points, respectively). The shaded region covers 80% of the tested spectral pulse power.

4. Experimental results

In Fig. 4, we show the group delay (and/or the spectral phase) measurement setup which we used in the following proof-of-concept experiment. We have built a fiber-ring laser with nonlinear polarization rotation mode-locking emitting at ~1560 nm with a frequency of 960 kHz. The details of this laser can be found in Ref. [24]. Next, we used an optical spectrum analyzer to measure the intensity spectrum of the pulse under test, i.e. $|F(\omega)|^2$, using a 50/50 fiber optic coupler. On the other hand, we also measured the intensity spectrum of the quadratically phase modulated signal $\left|F_{\phi_{20}}(\omega)\right|^2$. We used an electro-optic phase modulator (EO PM) ($LiNbO_3$, 12 GHz bandwidth) as a time lens. This EO PM was driven by an ultra-high-speed electrical pulse generator able to provide electric pulses at a maximum repetition rate of 1 MHz, a maximum voltage of 10 V (at 50 Ω), and with a minimum pulse width of 200 ps. This electrical pulse generator was in turn triggered by the same output light pulses from the laser under test via a photodetector. The tandem of ultra-high-speed electrical pulse generator/digital delay/pulse generator was necessary to synchronize the phase modulation with the passage of the light pulse under test through the modulator. This time synchronization was possible using the oscilloscope also shown in the figure, by selecting the time delay until the two signals overlap on the screen. For this reason we feed the phase modulator with an ultrashort electrical pulse generator rather than a sinusoidal signal. It is also important to note that the energy of both spectra should be equalized before applying Eqs. (13) to (15), since this type of transformation preserve the signal energy. Fortunately, it is not necessary to experimentally equalize the energy of the signals, since both operations can be more easily performed in the numerical stage. In contrast to the time-domain counterpart, where the time delays between pulse' profiles may need to be corrected numerically [12], here a spectral shift should not be present *a priori*, since the laser emits at a fixed central wavelength. It should be noted that Fig. 4 purports that both spectra, $|F(\omega)|^2$ and $\left|F_{\phi_{20}}(\omega)\right|^2$, could be measured simultaneously, which is not possible with our setup because the available optical spectrum analyzers (OSAs) usually have only one optical input. Therefore, both spectral measurements must be performed sequentially. In this case, there is a possibility of a small spectral shift between the spectral measurements (typically on the order of the OSA wavelength accuracy, i.e., 10 pm). However, if some

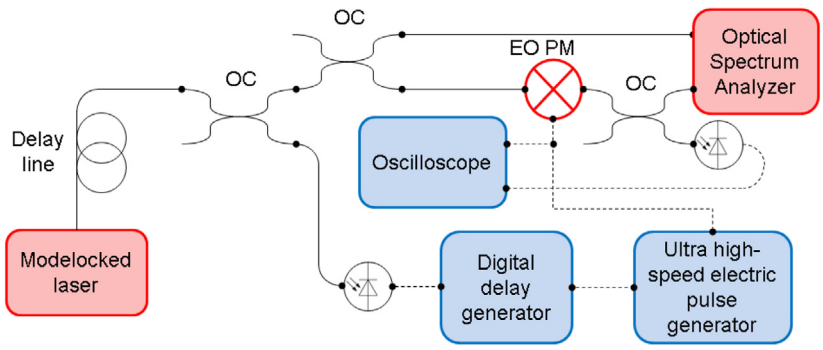

Fig. 4. Experimental setup, where OC: 50/50 optical couplers, EO PM: electro-optical phase modulator, solid curves: optical fibers, and dashed lines: electrical connections.

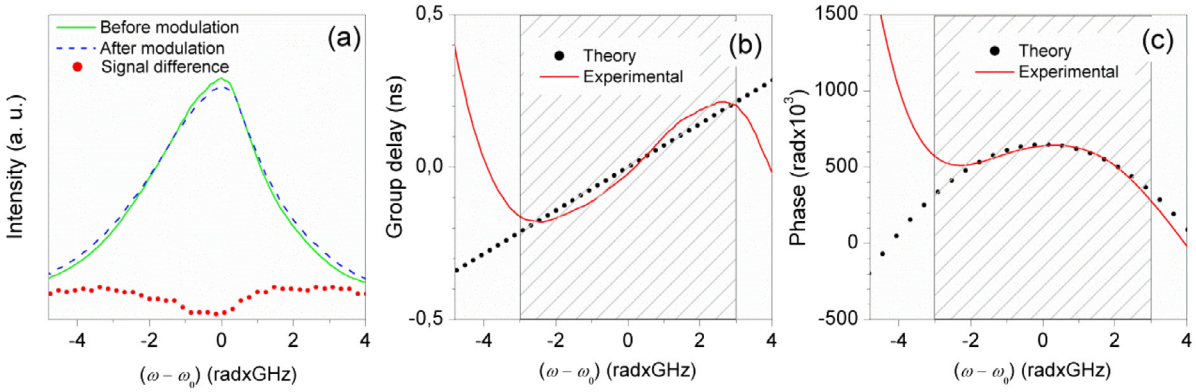

Fig. 5. (a) Measured intensity spectra of the tested pulse before and after quadratic phase modulation and the signal difference between them. (b) Determined spectral group delay and theoretical group delay according to Eq. (18). (c) Phase recovered by the proposed technique as compared with the theoretically determined. The shaded area focuses 90% of the tested spectral input power.

spectral shift is required to align the spectra, this can be done in the numerical step. Finally, as we have shown in the previous section, this system proved to be robust to the presence of noise, the use of different phase modulation factors, or a temporal mismatch between the pulse peak and the quadratic phase modulation in the time lens. Therefore, we will focus on the main aspect of this proof-of-concept experiment in the following.

We chose this particular laser configuration because it can generate a low-repetition-rate of soliton pulses depending on the pump power and the position of the fiber-paddle polarization control located in the resonator [24]. It is well known that a soliton is transform limited, i.e., there is a constant group delay in its optical spectrum, namely $\Phi'(\omega) = 0$. However, if we propagate these pulses along a delay line with certain length z and a certain dispersion parameter β_{20}, these light pulses will acquire a nonzero group delay given by:

$$\Phi'(\omega) = -\beta_{20} z \left(\omega - \omega_0\right); \tag{18}$$

which is given by Fourier transform of Eq. (3.2.9) in Ref. [23], where $(\omega - \omega_0)$ is the baseband angular frequency and ω_0 is the central optical frequency of emission. Therefore, we propagate transform-limited solitons with a full-width at half-maximum of 0.92 ps at 960 kHz over a 3.2 km delay line (SMF28 optical fiber) with a group velocity dispersion of -22.2 ps ^{2}/km at 1564.3 nm. The electric pulses produced by the ultra-high-speed electrical pulse generator were at the same repetition rate of the laser under test (960 kHz), with a peak voltage of 6.5 V (at 50 Ω), and with a pulse width of 230 ps. By fitting the electrical impulse used to drive the quadratic phase modulator to the time squared phase response given by Eq. (3), and considering the V_π of the EO PM, we estimated a $\phi_{20} \cong 5.4 \times 10^{20}$ rad × Hz^2. Fig. 5(a) shows the measured spectra before and after the quadratic phase modulation, i.e. $|F(\omega)|^2$ and $\left|F_{\phi_{20}}(\omega)\right|^2$, respectively, as well as the signal difference $\left|F_{\phi_{20}}(\omega)\right|^2 - |F(\omega)|^2$. Fig. 5(b) show the recovered group delay compared to the theoretical group delay given by Eq. (17); while in Fig. 5(c) we show the recovered spectral phase, obtained by using Eq. (14), as compared to the theoretical phase. In both cases, there is a reasonable level of agreement between the two profiles when $|\omega - \omega_0| \leq 3$ rad × GHz, which focuses 90% of the tested spectral input power.

5. Conclusions

We have discussed here a method to determine both the group delay and the phase of a given pulse in the Fourier optics domain. We first rederived a theoretical relationship between the group delay/phase and the spectral intensities before and after a given quadratic phase modulation, which provides a simpler route based on basic properties of the Fourier transform. The proposal is supported by several numerical results and a proof-of-concept experiment, with particular attention paid to the robustness of this technique by simulating additive and independent white noise.

Declaration of competing interest

The authors declare that they have no known competing financial interests or personal relationships that could have appeared to influence the work reported in this paper.

Acknowledgments

This work was supported in part by the European Union, project IPN-Bio (Ref.: H2020-MSCA-RISE-2019-872049), and by the *Generalitat Valenciana* of Spain (Ref.: PROMETEO/2019/048). C. Cuadrado-Laborde acknowledges the financial support from project PIP 2015-0607 (CONICET, Argentina). All authors approved the version of the manuscript to be published.

References

[1] T. Huang, J. Burnett, A. Deczky, The importance of phase in image processing filters, IEEE Trans. Acoust. Speech, Signal Process. 23 (1975) 529–542, http://dx.doi.org/10.1109/TASSP.1975.1162738.

[2] A. Oppenheim, J. Lim, G. Kopec, S. Pohlig, Phase in speech and pictures, in: IEEE Int. Conf. on Acoustics, Speech, and Signal Processing, ICASSP '79, 1979, pp. 632–637, http://dx.doi.org/10.1109/ICASSP.1979.1170798.

[3] M. Shechtman, Phase retrieval with application to optical imaging: A contemporary overview, IEEE Sign. Proc. Mag. 32 (2015) 87–109, http://dx.doi.org/10.1109/MSP.2014.2352673.

[4] A.V. Oppenheim, J.S. Lim, The importance of phase in signals, Proc. IEEE 69 (1981) 529–541, http://dx.doi.org/10.1109/PROC.1981.12022.

[5] D.J. Kane, R. Trebino, Characterization of arbitrary femtosecond pulses using frequency-resolved optical gating, IEEE J. Quantum Electron. 29 (1993) 571–579, http://dx.doi.org/10.1109/3.199311.

[6] C. Iaconis, I.A. Walmsley, Spectral phase interferometry for direct electric-field reconstruction of ultrashort optical pulses, Opt. Lett. 23 (1998) 792–794, http://dx.doi.org/10.1364/OL.23.000792.

[7] D.N. Fittinghoff, J.L. Bowie, J.N. Sweetser, R.T. Jennings, M.A. Krumbügel, K.W. DeLong, R. Trebino, I.A. Walmsley, Measurement of the intensity and phase of ultraweak, ultrashort laser pulses, Opt. Lett. 21 (1996) 884–886, http://dx.doi.org/10.1364/OL.21.000884.

[8] M. Miranda, T. Fordell, C. Arnold, A. L'Huillier, H. Crespo, Simultaneous compression and characterization of ultrashort laser pulses using chirped mirrors and glass wedges, Opt. Express 20 (2012) 688–697, http://dx.doi.org/10.1364/OE.20.000688.

[9] J.R. Fienup, Phase retrieval algorithms: A comparison, Appl. Opt. 21 (1982) 2758–2769, http://dx.doi.org/10.1364/AO.21.002758.

[10] L. Taylor, The phase retrieval problem, IEEE Trans. Antennas and Propagation 29 (1981) 386–391, http://dx.doi.org/10.1109/TAP.1981.1142559.

[11] R.W. Gerchberg, W.O. Saxton, A practical algorithm for the determination of phase from image and diffraction plane pictures, Optik 35 (1972) 237–246.

[12] C. Cuadrado-Laborde, A. Carrascosa, P. Pérez-Millán, A. Díez, J.L. Cruz, M.V. Andres, Phase recovery by using optical fiber dispersion, Opt. Lett. 39 (2014) 598–601, http://dx.doi.org/10.1364/OL.39.000598.

[13] C. Cuadrado-Laborde, I. Armas-Rivera, A. Carrascosa, E.A. Kuzin, A. Díez, M.V. Andrés, Instantaneous frequency measurement of dissipative soliton resonant light pulses, Opt. Lett. 41 (2016) 5704–5707, http://dx.doi.org/10.1364/OL.41.005704.

[14] C. Dorrer, I. Kang, Complete temporal characterization of short optical pulses by simplified chronocyclic tomography, Opt. Lett. 28 (2003) 1481–1483, http://dx.doi.org/10.1364/OL.28.001481, Principio del formulario.

[15] C. Dorrer, I.A. Walmsley, Concepts for the temporal characterization of short optical pulses, EURASIP J. Adv. Signal Process. 2005 (2005) 287905, http://dx.doi.org/10.1155/ASP.2005.1541.

[16] I.A. Walmsley, C. Dorrer, Characterization of ultrashort electromagnetic pulses, Adv. Opt. Photon. 1 (2009) 308–437, http://dx.doi.org/10.1364/AOP.1.000308.

[17] J. van Howe, C. Xu, Ultrafast optical signal processing based upon space-time dualities, J. Lightwave Technol. 24 (2006) 2649–2662, http://dx.doi.org/10.1109/JLT.2006.875229.

[18] V. Torres-Company, J. Lancis, P. Andrés, Chapter 1 space-time analogies in optics, in: E. Wolf (Ed.), Progress in Optics, Vol. 56, Elsevier, 2011, pp. 1–80, http://dx.doi.org/10.1016/B978-0-444-53886-4.00001-0.

[19] M.J. Bastiaans, K.B. Wolf, Phase reconstruction from intensity measurements in linear systems, J. Opt. Soc. Amer. A 20 (2003) 1046–1049, http://dx.doi.org/10.1364/JOSAA.20.001046.

[20] B.H. Kolner, Space–time duality and the theory of temporal imaging, IEEE J. Quantum Electron. 30 (1994) 1951–1963, http://dx.doi.org/10.1109/3.301659.

[21] C.V. Bennett, B.H. Kolner, Principles of parametric temporal imaging, I. System configurations, IEEE J. Quantum Electron. 36 (2000) 430–437, http://dx.doi.org/10.1109/3.831018.

[22] C. Dorrer, Effect of jitter on linear pulse-characterization techniques, Opt. Express 16 (2008) 6567–6578, http://dx.doi.org/10.1364/OE.16.006567, Principio del formulario.

[23] G.P. Agrawal, Nonlinear Fiber Optics, third ed., Academic Press, 2001.

[24] C. Cuadrado-Laborde, J.L. Cruz, A. Díez, M.V. Andrés, Sub-picosecond ultra-low frequency passively mode-locked fiber laser, Appl. Phys. B 122 (2016) 273, http://dx.doi.org/10.1007/s00340-016-6548-z.